BioSystems 103 (2011) 79–84

Contents lists available at ScienceDirect

BioSystems

journal homepage: www.elsevier.com/locate/biosystems

Up-and-down movement of a sliding actin filament in the *in vitro* motility assay

Itsuki Kunita [a], Shigeru Sakurazawa [b,*], Hajime Honda [c]

[a] Molecular and System Life Science Unit, Riken Advanced Science Institute, 2-1 Hirosawa, Wako-shi, Saitama 351-0198, Japan
[b] School of Systems Information Science, Future University Hakodate, 116-2 Kamedanakano, Hakodate, Hokkaido 041-8655, Japan
[c] Department of BioEngineering, Nagaoka University of Technology, 6000 Kamitomioka, Nagaoka, Niigata 940-2188, Japan

ARTICLE INFO

Article history:
Received 25 August 2010
Received in revised form 3 October 2010
Accepted 5 October 2010

Keywords:
Actin filament
Sliding movement
In vitro motility assay
Evanescent field fluorescent microscopy

ABSTRACT

We observed a three-dimensional up-and-down movement of an actin filament sliding on heavy meromyosin (HMM) molecules in an *in vitro* motility assay. The up-and-down movement occurred along the direction perpendicular to the planar glass plane on which the filament demonstrated a sliding movement. The height length of the up-and-down movement was measured by monitoring the extent of diminishing fluorescent emission from the marker attached to the filament in the evanescent field of attenuation. The height lengths whose distribution exhibits a local maximum were found around the two values, 150 nm and 90 nm, separately. This undulating three-dimensional movement of an actin filament suggests that the interactions between myosin (HMM) molecules and the actin filament may temporally be modulated during its sliding movement.

1. Introduction

There has already been accumulated a sufficient amount of investigations focusing upon the mechanisms of force generation driving muscle contraction. That is interactions between actin and myosin molecules (Huxley and Niedergerke, 1954; Huxley and Hanson, 1954; Huxley, 1969; Huxley and Simmons, 1971; Yanagida et al., 1985; Yanagida, 1990; Harada et al., 1990; Pollack, 1996). Fluorescent microscope technique in the framework of *in vitro* motility assay enables one to directly observe the sliding movement of actin filaments on HMMs fixed on the glass surface (Yanagida et al., 1984; Honda et al., 1986; Kron and Spudich, 1986; Harada et al., 1987; deBeer et al., 1997). The movement has been supposed to smoothly be planar on the glass surface.

However, each molecular state appearing in one cycle of ATP hydrolysis has a three-dimensional structure that is stereochemical. In fact, the binding between an actin molecule and a myosin head is complementary with each other in their conformations under rigor conditions and the attachment is complete there (Rayment et al., 1993). Conformational changes in the actin–HMM complex that occur during the sliding movement could be visually monitored by quick-freeze deep-etch electron microscopy (Katayama, 1998). The results revealed that a limited number of HMM heads are in the state of rigor conformation, while most of the heads form ATP-bound crossbridges. Moreover, the direct measurements of the force generated in single actin filaments demonstrate that the interactions necessary for the force generation were implemented in a very limited number of myosin molecules (Nishizaka et al., 1995). These observations, when combined together, come to suggest that the interactions necessary for the force generation for the sliding movement may be quite sporadic between actin molecules and HMM heads. We shall then examine how intermittent spatio-temporally the interactions could be between actin and myosin for the generation of the force for driving the sliding movement of an actin filament.

For this objective, we employed the method of evaluating the exponential decrease of evanescent light-intensity to estimate the extent to which an actin filament could move in the direction perpendicular to the planar plane of the sliding movement. The vertical displacement of the filament was measured as focusing upon the fluorescent marker or as utilizing a speckled actin filament in order to gain a high spatial resolution (Honda et al., 1999).

2. Materials and methods

2.1. Proteins

Actin and myosin were extracted from rabbit skeletal muscle (Spudich and Watt, 1971; Perry, 1955). HMM was prepared by alpha-chymotryptic digestion of myosin (Okamoto and Sekine, 1985). In order to observe an actin filament, two kinds of the fluorescence-labeled actin filaments, totally labeled actin filaments and speckled actin filaments, were prepared. Totally labeled actin filament was made and treated with equal molar rhodamin-phalloidin (Sigma) in buffer A (25 mM KCl, 25 mM imidazole–HCl, 3 mM $MgCl_2$, 1 mM DTT, pH = 7.4). In order to prepare speckled actin filaments, G-actin and equal molar phalloidin (Sigma) was mixed in buffer A, and was added to the solution containing segmented fluorescence-labeled actin filaments. The mixture was placed at a temperature of 4 °C for 12 h for formation of the speckled actin filaments.

* Corresponding author. Tel.: +81 138 34 6335; fax: +81 138 34 6301.
E-mail address: sakura@fun.ac.jp (S. Sakurazawa).

0303-2647/$ – see front matter © 2010 Elsevier Ireland Ltd. All rights reserved.
doi:10.1016/j.biosystems.2010.10.005

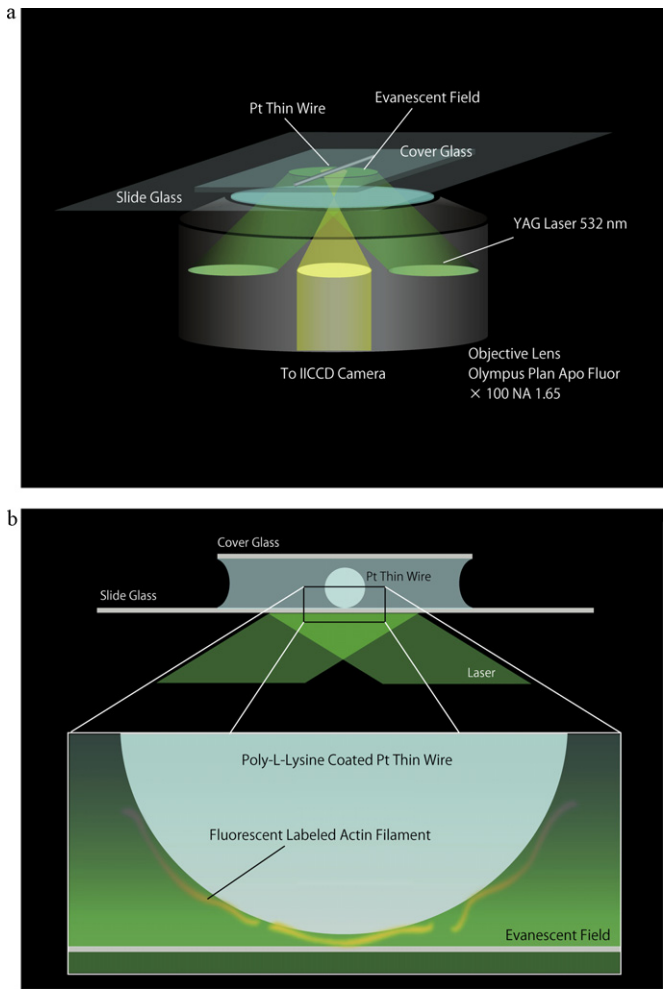

Fig. 1. (a) Schematic diagram of determination system of intensity–height transformation curve by using Pt wire, labeled actin filament and TIRFM. (b) Height estimation of actin filaments observed by TIRFM. The luminance of actin filaments adsorbed to Pt wire with a round cross section darkened exponentially with increasing the distance from glass surface based on a curvature of Pt wire.

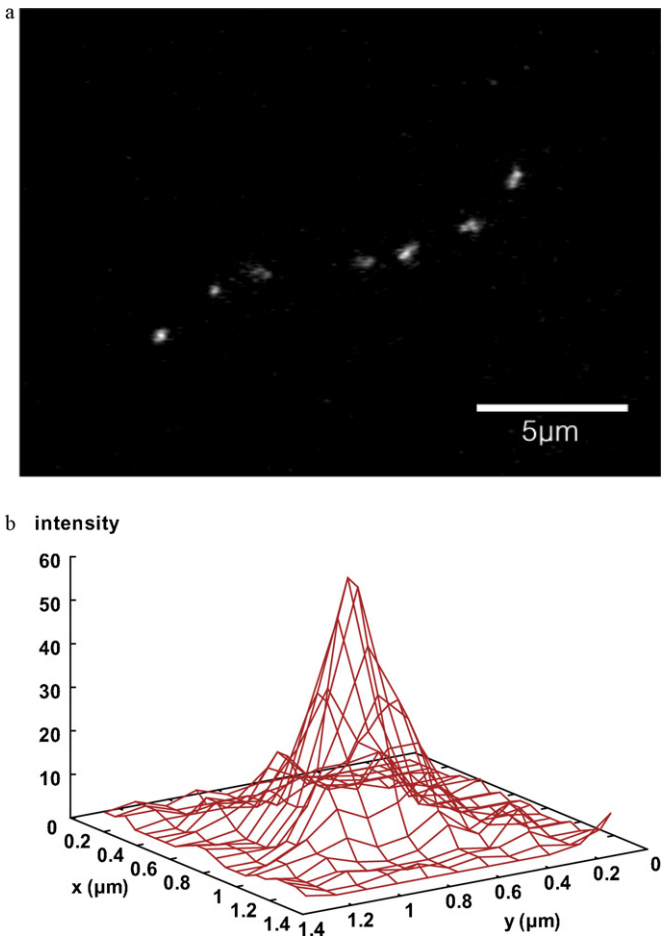

Fig. 2. (a) A typical image of a single speckled actin filament consisted of seven fluoresce-labeled spots observed with TIRFM. Each spots were sliding on surface-fixed HMMs by forming line longitudinally. (b) Intensity profile of a fluorescence-labeled spot on the actin filament. The intensity means the grayscale intensity values. The profile had 2D-Gaussian distribution. From the fitting function of the Gaussian, the position of the spot is determined as the *x*–*y* coordinate of the top.

2.2. Observations

The microscope (Olympus, IX70) attached with the objective lens (Olympus, Apo 100×, oil, NA = 1.65) was used for the fluorescence-labeled actin filaments with total reflection illumination unit (Olympus, IX2-RFAEVA). A diode pumped frequency doubled Nd:Yag laser (JDS Uniphase, Model 4611-010-0980) was used as the light source for a total internal reflection fluorescence microscopy (TRIFM). Images under the microscope were taken with an image-intensified CCD camera (Hamamatsu Photonics, C2400-97V) and recorded in a hard disk through a video capture board (I-O DATA, GV-BCTV5/PCI). Each image was captured at every 1/30 s.

In order to measure the planarity of the collodion-coated glass surface, the surface of collodion film was scanned as using a tapping mode atomic force microscopy (AFM, Veeco: Multi Mode AFM). The AFM results were recorded with software (Veeco: NanoScope Control, NanoScope Image), and analyzed with software (Image Metrology: SPIP).

2.3. Determination of intensity–height transformation curve

The height of actin filaments in the evanescent light was determined from the intensity with use of a Pt wire (see Fig. 1). The Pt wire (ϕ = 0.3 mm) were treated with poly-L-lysine (Sigma Co.). The totally labeled actin filaments adsorbed to the Pt wire were observed by TIRFM, and the images were recorded.

The relationship between the height of an actin filament and the light intensity was calculated from the curvature of the Pt wire, and estimated a laser incident angle from the theoretical values available in the following equation (Axelrod, 2003).

$$I(z) = I(0)\exp\left(\frac{-z}{d}\right)$$
$$d = \frac{1}{2k_2}\left\{\frac{1}{n}\sqrt{\sin^2\theta - n^2}\right\}^{-1} \quad (1)$$

The intensity of the evanescent field exponentially decays with the perpendicular distance z. Parameter k_2 (=$2\pi/\lambda$) here is the wavenumber of the incident laser in the solution, n is relative refractive index of the solution to the glass, and θ is the incident angle of the laser beam. An intensity–height transformation curve was determined based on theoretical values on the incident angle.

2.4. In vitro motility assay

We prepared a standardized *in vitro* motility assay (Hatori et al., 1998, 1996). The slide glass to fix HMM was hydrophobically treated with 0.1% collodion (nacalaitesque) in 3-methylbutyl acetate. The solution condition for observing the sliding movement of an actin filament was 25 mM KCl, 25 mM imidazole–HCl (pH = 7.4), 3 mM $MgCl_2$, 0–2 mM ATP, and 0.5% β-mercaptoethanol at 22 °C.

2.5. Image analysis

In order to remove the unevenness of illumination and offset of the camera, all images were corrected with the correction coefficient. The coefficient was determined by observing the images of rhodamine dispersed uniformly on the glass surface. A specimen of rhodamine was dissolved in the solution for *in vitro* motility assay.

The position of each spotted marker along an actin filament was determined as reading the light intensity distribution from the marker (see Fig. 2). The height was estimated from the intensity–height transformation curve.

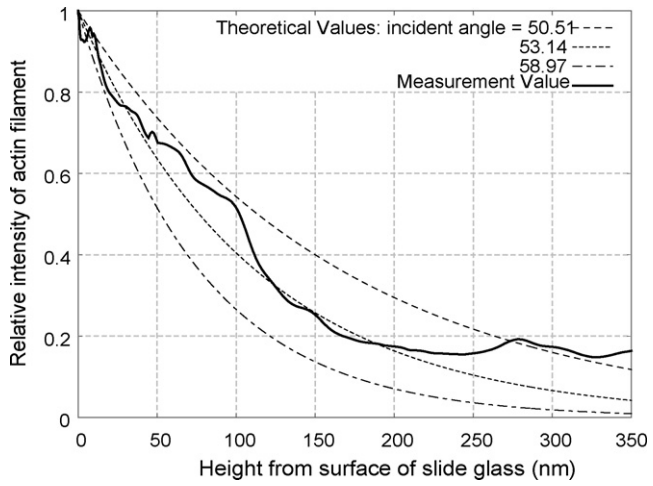

Fig. 3. Intensity profile of fluorescence-labeled actin filament adsorbed to Pt wire (solid line) and the theoretical values (dashed line). The refractive index $n = 0.7472$ and the wave number $k_2 = 0.0157$ were assumed here, and the theoretical values were calculated (see Eq. (1)).

3. Results and discussion

3.1. Measurement of the height from the total reflection surface using evanescent light attenuation

To monitor the sliding movement of an actin filament in the three-dimensional space, the position giving the locally maximum light intensity of the labeled actin filament was focused upon as a measure for estimating their height elevated from the total reflection surface. Fig. 3 displays a relationship between the light intensity of the labeled actin filaments adsorbed to the Pt wire surface and the height from the total reflection surface. The height was estimated from the curvature of the cross section surface of Pt wire. The measured value was almost identical to the theoretical counterpart, which was determined by the incident angle of the laser beam. The feasible incident angle was adjusted to 51.98° so as to minimize the difference between the actual measurement and the theoretical estimate. The correlation coefficient was 0.912256.

3.2. Evaluation of feasibility of 3D observation system

We first monitored the vertical fluctuations of an actin filament in the absence of ATP for evaluating the feasibility of this system. An actin filament fixed on HMMs was observed by the two independent methods. One was by total reflection, and the other by incident illumination as setting the incident angle to be less than the critical angle. The images observed by the two methods were remarkably different as demonstrated in Fig. 4. Although the observed light intensity of the filament under incident illumination was uniform, it was not uniform under total reflection illumination. The fading rate of fluorescent signals was estimated $-0.56 \pm 0.18\%/s$, as implying that the effect of the fading was sufficiently insignificant during our observations. Unevenness of the illumination and offset of the camera were adjusted in advance by checking the sample images of the glass on which rhodamine was dispersed uniformly. We also minimized the contributions from the interference fringes. The present setup enabled us to prepare the dark regions by changing the incident angle beyond the scope of the total reflection illumination.

Fig. 5 displays a relationship between the temporal averages of the elevated height of a spotted marker attached on an actin filament and their standard deviations. The average of the vertical displacement was found over the range from 100 nm to 450 nm. The standard deviation increased with the increase of the average.

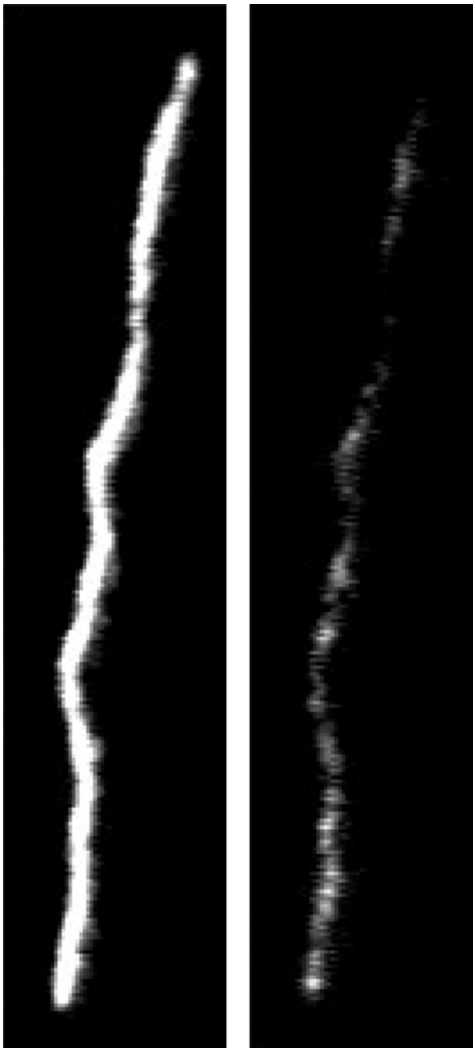

Fig. 4. Fluorescence images of an all labeled actin filaments observed by incident illumination (left) and the total reflection illumination (right). This actin filament was fixed on HMM (0.045 mg/ml) in the absence ATP.

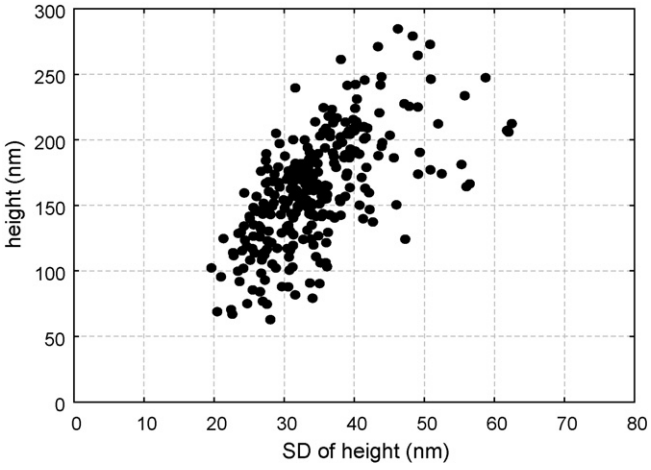

Fig. 5. The relationship between the temporal standard deviations and the temporal averages of the height of fluorescent-labeled spots on actin filaments fixed on HMMs (0.045 mg/ml) in the absence of ATP.

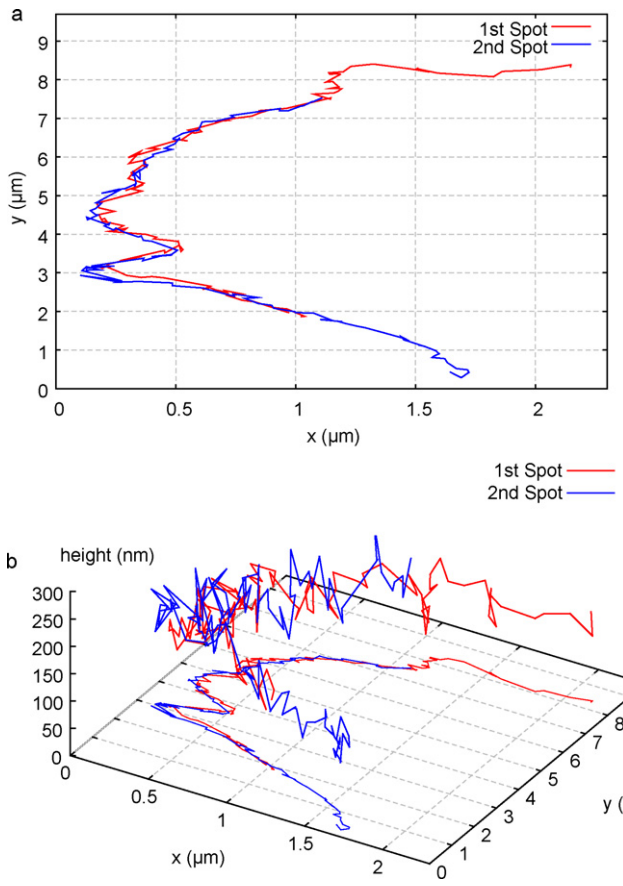

Fig. 6. 2D and 3D trajectories of two spotted markers, red and blue, attached to an actin filament sliding on HMMs (0.045 mg/ml) fixed on the glass surface in the presence of 0.05 mM ATP. The separation between the two spots was 1.65 μm.

The planarity of the collodion-coated surface was examined by atomic force microscopy under dry condition. The standard deviation of the measured thickness was 0.45 nm, which remained sufficiently insignificant in influencing our measurement of the height distance.

As Katayama (1998) has already pointed out, it is quite infrequent that the portions of HMMs attaching an actin filament could exist in rigor state. This observation comes to suggest to us that the lowest height position displayed in Fig. 5 could be fixed on HMMs. It could also be likely that portions of an actin filament at a higher elevation may move rather freely without attaching to HMMs. This is a case for those enhanced fluctuations associated with the 3D movement of an actin filament.

3.3. Observation of actin filaments during sliding movement

We observed the 3D movement of an actin filament sliding on HMMs in the presence of ATP to be hydrolyzed. Fig. 6 displays the trajectory of each marker spot on an actin filament. It was then found that the sliding actin filaments were flexible and could fluctuate not only horizontally but also vertically. Fig. 7 demonstrates typical time developments of the height trajectory of a spotted marker both in the absence and in the presence of ATP. The averaged height distance of an actin filament during its sliding movement in the presence of ATP was 150 nm, while the height was shortened down to 90 nm from time to time. In the absence of ATP, on the other hand, the height distance from the glass surface was maintained at about 90 nm. On the other hand, the estimated height of the filament in the absence of ATP was about 90 nm from the glass surface. Considering the total length of HMM of about 60 nm and

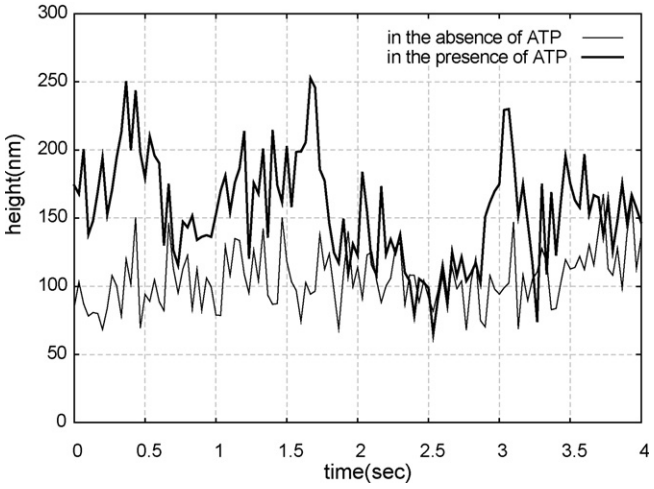

Fig. 7. Time development of the height of a fluorescence-labeled spot in the absence of ATP (thin line) and in the presence of 0.02 mM ATP (thick line). In the absence of ATP, the marker fluctuated over the range from 70 nm to 150 nm in the distance length, and exhibited a Brownian motion. In the presence of ATP, the markers were sliding on HMMs (0.045 mg/ml) fixed to the glass surface, and fluctuated over the range from 90 nm to and 250 nm heights. The height distance was lowered down to 100 nm from time to time.

the thickness of the collodion film placed under the HMM layer, it could be inferred that the height distance 90 nm of the filament in the absence of ATP may correspond to the length of a head-top of a HMM. It thus would become hard for a HMM to make a direct contact to an actin filament while the filament maintains the height distance to be 150 nm during its sliding movement.

According to the previous report (Honda et al., 1999), it is possible that an actin filament exhibits contractile distortions during its sliding movement. Considering that the extent of contractile distortions was as much as 10% of the total length of the filament, we could estimate that fluctuations due to the vending displacement of the filament may reach over 100 nm in the direction perpendicular to the sliding movement. To our best knowledge, this is the first experimental demonstration of a three-dimensional structure of the spatio-temporal interactions operating between HMM molecules and an actin filament during its sliding movement.

3.4. Near-field and far-field interactions between an actin filament and HMMs

For the purpose of studying the nature of the dynamics underlying the induction of the changes in the height distance of an actin filament, we further examined the correlation of two separate markers attached to the filament, the 1st spot and 2nd spot, as depicted in Fig. 8a and b. Fig. 8a displays the time points, denoted as drop points, at which the height distance of 1st spot reaches a local minimum, in which each local minimum distance was identified by averaging the distances measured at three adjacent time points. Fig. 8b is the similar for 2nd spot. Fig. 9 actually exhibits a close correlation between the 1st and 2nd spot in the respect that the points of local minimum height distance occurred almost at the same locations for both the 1st and 2nd spot on the two-dimensional plane for the sliding movement. Fig. 10 displays a spatial correlation of the variations in the height distance between the 1st and 2nd spot, and reveals that the occurrence of the local minimum height distance likely coincides with that of a high spatial correlation of the variations in the height distance between the two spots. This observation, when combined with the length of the head-top of a HMM roughly of 60 nm, suggests that the contact interaction between an actin filament and HMMs may take place where the occurrence of

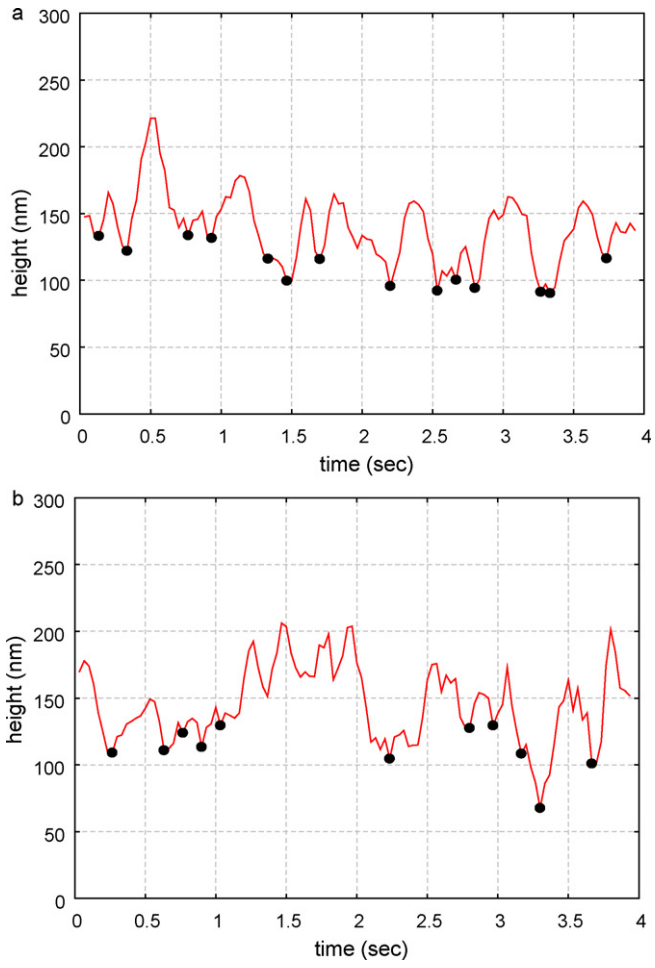

Fig. 8. Time development of the height distance of each marker.

a local minimum height distance spatially overlaps with that of a high spatial correlation of the variations in the height distance.

Furthermore, we evaluated the extent to which the present observations may depend upon the total length of an actin filament to be examined. We then prepared actin filaments with various total lengths ranging from 100 nm to 10 μm and conducted the similar experiments. The results revealed that all of the specimens demonstrate the similar behaviors as experienced with the original

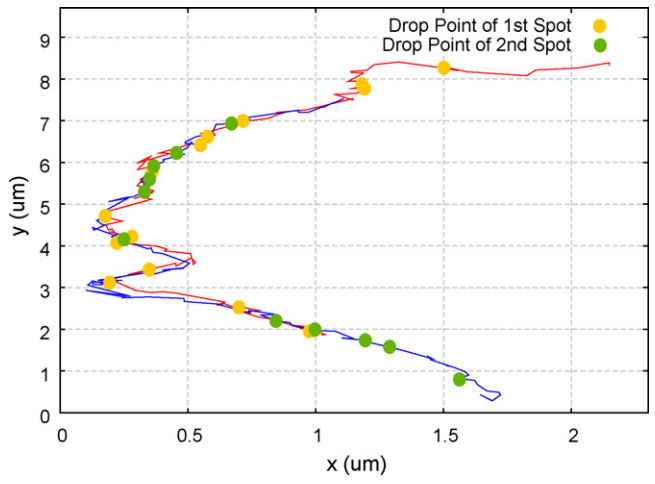

Fig. 9. Two-dimensional trajectories of the spatial point at which the height distance reaches a local minimum.

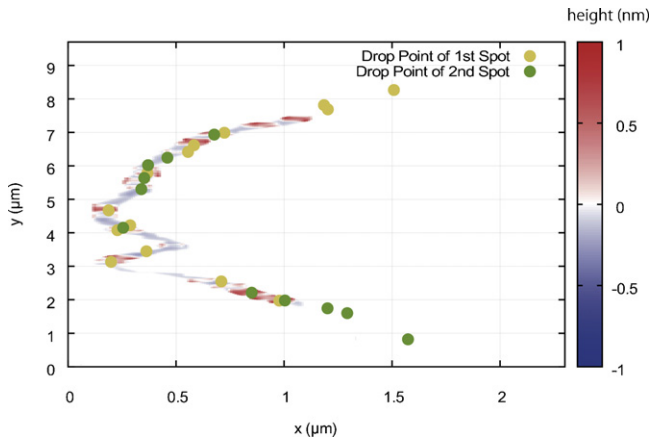

Fig. 10. A spatial correlation of the variations in the height distance between the 1st and 2nd spot, and reveals that the occurrence of the local minimum height distance likely coincides with that of a high spatial correlation of the variations in the height distance between the two spots.

sample with two distinct markers. Namely, the distribution of the height distances was observed to have a local minimum at two distinct distances, 90 nm and 150 nm. The relative frequency for the distribution centered at 150 nm was almost 4 times greater than that centered at 90 nm.

The observed fact of an actin filament detached from HMM molecules even during its sliding movement as being involved in the bending displacement in the direction perpendicular to the planar movement provides us with a new picture for the interpretation of the underlying molecular interactions. In addition to the near-field interactions regulating the contact between an actin filament and myosin molecules, there must also be a contribution from the far-field interactions causing the filament to be detached from myosin molecules and to participate in a filamental bending displacement.

Acknowledgements

We appreciate helpful discussions with Professor Koshin Mihashi of Nihon Fukushi University. We owed the measurement with use of AFM to Professor Toshio Ando and Dr. Susumu Nitta of Kanazawa University.

References

Axelrod, D., 2003. Total internal reflection fluorescence microscopy in cell biology. Methods Enzymol. 361, 1–33.
deBeer, E.L., Sontrop, A.M.A.T.A., Kellermayer, M.S.Z., Galambos, C., Pollack, G.H., 1997. Actin-filament motion in the in vitro motility assay has a periodic component. Cell Motil. Cytoskeleleton 38, 341–350.
Harada, Y., Noguchi, A., Kishino, A., Yanagida, T., 1987. Sliding movement of single actin filaments on one-headed myosin filaments. Nature 326, 805–808.
Harada, Y., Sakurada, K., Aoki, T., Thomas, D.D., Yanagida, T., 1990. Mechanochemical coupling in actomyosin energy transduction studied by in vitro movement assay. J. Mol. Biol. 216, 49–68.
Hatori, K., Honda, H., Shimada, K., Matsuno, K., 1998. Propagation of a signal coordinating force generation along an actin filament in actomyosin complex. Biophys. Chem. 75, 81–85.
Hatori, K., Honda, H., Matsuno, K., 1996. ATP-dependent fluctuations of single actin filaments in vitro. Biophys. Chem. 58, 267–272.
Honda, H., Nagashima, H., Asakura, S., 1986. Directional movement of F-actin in vitro. J. Mol. Biol. 191, 131–133.
Honda, H., Hatori, K., Igarashi, Y., Shimada, K., Matsuno, K., 1999. Contractile and protractile coordination with in an actin filament sliding on myosin molecules. Biophys. Chem. 80, 139–143.
Huxley, A.F., Niedergerke, R., 1954. Structural changes in muscle during contraction: interference microscopy of living muscle fiber. Nature 173, 971–973.
Huxley, H.E., Hanson, J., 1954. Changing in the cross-striations of muscle during contraction and stretch and their structural interpretation. Nature 173, 973–976.
Huxley, H.E., 1969. The mechanism of muscular contraction. Science 164, 1356–1366.

Huxley, A.F., Simmons, R.M., 1971. Proposed mechanism of force generation in striated muscle. Nature 233, 533–538.
Katayama, E., 1998. Quick-freeze deep-etch electron microscopy of the actin-heavy meromyosin complex during the in vitro motility assay. J. Mol. Biol. 278, 349–367.
Kron, S.J., Spudich, J.A., 1986. Fluorescent actin filaments move on myosin fixed to a glass surface. PNAS 83, 6272–6276.
Nishizaka, T., Miyata, H., Yoshikawa, H., Ishiwata, S., Kinosita, K., 1995. Unbinding force of a single motor molecule of muscle measured using optical tweezers. Nature 377, 251–254.
Okamoto, Y., Sekine, T., 1985. A streamlined method of subfragment one preparation from myosin. J. Biochem. 98, 1143–1145.
Perry, S.V., 1955. Myosin adenosinetriphosphatase. Methods Enzymol. 2, 288–582.
Pollack, G.H., 1996. Phase transitions and the molecular mechanism of contraction. Biophys. Chem. 59, 315–328.
Rayment, I., Holden, H.M., Whittaker, M., Yohn, C.B., Lorenz, M., Holmes, K.C., Milligan, R.A., 1993. Structure of the actin–myosin complex and its implications for muscle contraction. Nature 261, 58–65.
Spudich, J.A., Watt, S., 1971. The regulation of rabbit skeletal muscle contraction. J. Biol. Chem. 246, 4866–4871.
Yanagida, T., Nakase, M., Nishiyama, K., Oosawa, F., 1984. Direct observation of motion of single F-actin filaments in the presence of myosin. Nature 307, 58–60.
Yanagida, T., Arata, T., Oossawa, F., 1985. Sliding distance of actin filament induced by a myosin crossbridge during one ATP hydrolysis cycle. Nature 316, 366–369.
Yanagida, T., 1990. Loose coupling between chemical and mechanical reactions in atomyosin energy transduction. Adv. Biophys. 26, 75–95.